



Contents lists available at ScienceDirect

LWT

journal homepage: [www.elsevier.com/locate/lwt](http://www.elsevier.com/locate/lwt)

# AviTag-nanobody based enzyme immunoassays for sensitive determination of aflatoxin B<sub>1</sub> in cereal

Ting He<sup>a,b,\*,1</sup>, Tingting Yan<sup>a,c,1</sup>, Jiang Zhu<sup>a,c</sup>, Ying Li<sup>a,c</sup>, Xin Zhou<sup>a,c,d</sup>, Yunhuang Yang<sup>a,c,d,\*\*</sup>, Maili Liu<sup>a,c,d</sup>

<sup>a</sup> State Key Laboratory of Magnetic Resonance and Atomic Molecular Physics, Key Laboratory of Magnetic Resonance in Biological Systems, National Center for Magnetic Resonance in Wuhan, Wuhan National Laboratory for Optoelectronics, Wuhan Institute of Physics and Mathematics, Innovation Academy for Precision Measurement Science and Technology, Chinese Academy of Sciences, Wuhan, 430071, China

<sup>b</sup> Wuhan Academy of Agricultural Sciences, Wuhan, 430072, China

<sup>c</sup> University of Chinese Academy of Sciences, Beijing, 100049, China

<sup>d</sup> Optics Valley Laboratory, Hubei, 430074, China

## ARTICLE INFO

### Keywords:

Aflatoxin B<sub>1</sub>  
Nanobody  
Biotinylation  
Streptavidin  
Magnetic separation

## ABSTRACT

Aflatoxin B<sub>1</sub> (AFB<sub>1</sub>) is a well-known carcinogen for human health, and requires sensitive and rapid methods for monitoring. Here, we developed an Avi-tagged nanobody (AviTag-Nb) and incorporated it into the biotin-streptavidin-amplified ELISA (BA-ELISA) and magnetic bead-based ELISA (MB-ELISA) to detect AFB<sub>1</sub>. After optimization, BA-ELISA and MB-ELISA achieved 50% inhibitory concentrations (IC<sub>50</sub>) of 0.28 and 0.53 ng/mL, respectively, and provided results within 50 and 26 min, making them more sensitive and time-saving compared to the classic ELISA. The detection limits (LODs) of BA-ELISA and MB-ELISA were down to 0.07 and 0.12 ng/mL, respectively, ensuring their practical application in AFB<sub>1</sub> analysis. Additionally, both assays provided satisfactory recoveries (90.0%–97.2%) and favorable relative standard deviation (4.00%–10.5%) when tested with spiked cereal samples, aligning well with the results obtained from HPLC. Therefore, the AviTag-Nb shows promise as a valuable reagent in immunoassays, and the proposed BA-ELISA and MB-ELISA methods can serve as practical analytical tools for determining AFB<sub>1</sub> in real samples.

## 1. Introduction

Aflatoxins (AFs) are a group of occurring mycotoxins mainly produced by *Aspergillus flavus* and *A. parasiticus* in cereal grains (Okechukwu, Adelusi, Kappo, Njobeh, & Mamo, 2024). Among them, aflatoxin B<sub>1</sub> (AFB<sub>1</sub>) is the predominant form with the highest toxic potential, and has been classified as a group I human carcinogen (Ostry, Malir, Toman, & Grosse, 2017). Many countries have set action levels for AFB<sub>1</sub> in various food and feeds. For instance, the European Commission has defined the maximum permissible content of AFB<sub>1</sub> in human food as not exceeding 2 µg/kg (European Commission, 2010). The quantitative detection of AFB<sub>1</sub> through sensitive and rapid analytical techniques is crucial to mitigate AFB<sub>1</sub> contamination levels and associated health

risks. Currently, AFB<sub>1</sub> is commonly detected using instrument-based methods such as high-performance liquid chromatography (HPLC) and liquid chromatography tandem mass spectrometry (LC-MS/MS) (Wang, Chu, Qu, Ding, & Kang., 2024; Yoshinari et al., 2024). However, these methods require skilled technicians, long assay time, and cumbersome sample pretreatments, which largely limits their application in scenarios requiring rapid screening of a large number of samples. As an ideal alternative, antibody-mediated immunoassays (e.g., enzyme-linked immunosorbent assay (ELISA), immunochromatographic assay (ICA), and immunosensor), have been developed for mycotoxin screening with the advantages of simplicity, high throughput, cost effectiveness, and ease of automation (Chen et al., 2023).

High-quality antibodies are essential components of immunological

\* Corresponding author. Innovation Academy for Precision Measurement Science and Technology, Chinese Academy of Sciences, West No. 30 Xiao Hong Shan, Wuhan, 430071, China.

\*\* Corresponding author. Innovation Academy for Precision Measurement Science and Technology, Chinese Academy of Sciences, West No. 30 Xiao Hong Shan, Wuhan, 430071, China.

E-mail addresses: [ht210@apm.ac.cn](mailto:ht210@apm.ac.cn) (T. He), [yang\\_yh@apm.ac.cn](mailto:yang_yh@apm.ac.cn) (Y. Yang).

<sup>1</sup> These authors contributed equally to this work.

<https://doi.org/10.1016/j.lwt.2024.115858>

Received 29 August 2022; Received in revised form 7 February 2024; Accepted 10 February 2024

Available online 13 February 2024

0023-6438/© 2024 The Authors. Published by Elsevier Ltd. This is an open access article under the CC BY-NC-ND license (<http://creativecommons.org/licenses/by-nc-nd/4.0/>).

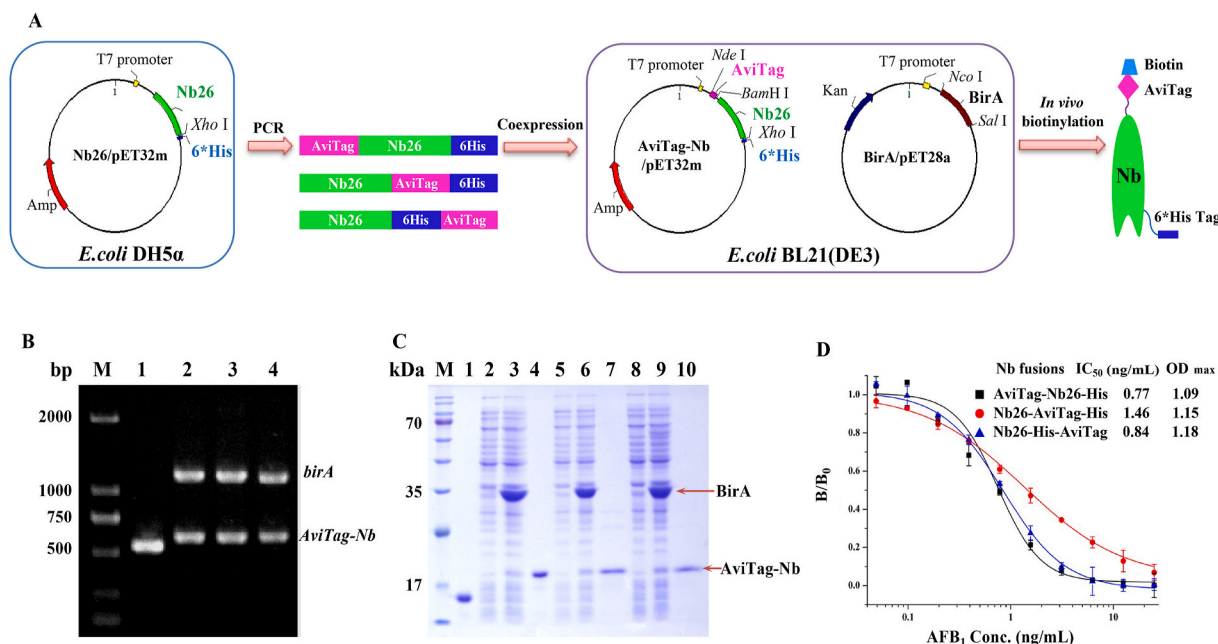


**Fig. 1.** Production and identification of biotinylated AviTag-Nb fusion proteins. (A) Schematic diagram of the construction of the expression plasmids for AviTag-Nb fusion proteins. (B) Agarose gel electrophoresis analysis of the colony PCR. Lane M: DL2000 DNA ladder; Lane 1: unfused Nb26 gene; Lanes 2–4: three colonies containing AviTag-Nb26-His and BirA genes (lane 2), Nb26-AviTag-His and BirA genes (lane 3), and Nb26-His-AviTag and BirA genes (lane 4). (C) SDS-PAGE. Lane M: protein marker; Lane 1: purified wide-type Nb26; Lanes 2, 5, and 8: whole-cell extracts under noinduced condition; Lanes 3, 6, and 9: whole-cell extracts after induction; Lanes 4, 7, and 10: purified biotinylated AviTag-Nb fusions. (D) Identification of the biotinylated AviTag-Nb fusions by iCELISA using SA-HRP as the detection tracer.

assay systems because they guarantee the analytical performance of an immunoassay. However, the biological activity of conventional polyclonal antibodies (pAbs) and monoclonal antibodies (mAbs) employed in the construction of an immunoassay can be easily influenced by chemical labeling reactions (e.g., labeling with peroxidase, nanoparticles, and other signal probes) (He et al., 2020; Zuo, Yan, Tang, Zhang, & Li, 2023), and also be susceptible to stringent conditions like high concentration of organic solvents and high temperatures (Cai et al., 2023; Liang et al., 2022). Driven by the growth of molecular engineering and phage display technology, the discovery of recombinant antibodies can provide new recognition elements (Guliy, Evstigneeva, & Dykman, 2023). The variable domain of heavy chain antibodies (VHHs), also known as nanobodies (Muyldermans, 2021), have received widespread attention due to their small size (~15 kDa), high expression yields, exceptional stability, and simplicity in genetic manipulation. More importantly, their single domain conformation facilitates the creation of different recombinant chimeric or tagged Nbs. Currently, several dual-functional nanobody fusions have been reported, including Nb-alkaline phosphatase (Yu et al., 2023), Nb-green fluorescent protein (Zuo, Yan, et al., 2023), Nb-luciferase (Wu et al., 2024), and Nb-streptavidin binding peptide (Mao et al., 2022), which can avoid the problems of decreasing antibody activity caused by random chemical modifications and reduce the use of secondary antibodies. Consequently, Nbs are extremely suitable for building robust and facile analytical methods for detecting small-molecule pollutants (Wang, Mukhtar, Ma, Pang, & Wang, 2018).

Recently, many efforts have been made to explore the application of Nb-based immunodetection approaches. Various signal amplification strategies, including the biotin-streptavidin (BS) system (Sun, Wang, Tang, Chen, & Liu, 2019), hybridization chain reaction (Liu et al., 2020), cascade enzyme amplification (Su et al., 2021), nanomaterial-mediated signal amplification (Li, Zhang, Zhang, Li, & Tang, 2023), and combined methods, have been employed to enhance the analytical performance. The BS system, in particular, has long been used to develop highly sensitive immunoassays due to the strong affinity between streptavidin

and biotin ( $K_d \approx 10^{-14} - 10^{-16}$  mol/L) (Yang et al., 2020). Relying on this system, we have exploited biotin binding with Nb in a chemical labeling manner, and a signal molecule of streptavidin-polyHRP conjugate was added, thereby catalyzing more substrates to generate more signals (Yan et al., 2022). Thus, the BS system offers an efficient method for AFB<sub>1</sub> detection. Recent studies have shown that Nb can readily fuse with the biotin receptor peptide AviTag to generate AviTag-Nb fusion protein, which can be biotinylated by BirA biotin ligase in *E. coli* (Chen et al., 2022). This strategy enables site-specific labeling of biotin, resulting in biotinylated Nbs with minimal batch-to-batch variation. However, there are limited reports on the application of AviTag-Nb fusion protein for developing anti-AFB<sub>1</sub> immunoassay, and this approach holds promise in utilizing its advantages in signal amplification to improve the analytical sensitivity of AFB<sub>1</sub> monitoring in food.

In this work, we proposed the use of AviTag/BirA technology to obtain a biotinylated AviTag-Nb. We then investigated its application in immunoassay development for AFB<sub>1</sub> detection. Two simple enzyme immunoassays, namely biotin-streptavidin-amplified ELISA (BA-ELISA) and magnetic bead-based ELISA (MB-ELISA), were established. The performance of these assays was evaluated in terms of sensitivity, selectivity, limit of detection, and working range. Finally, the accuracy and practicality of these two assays were confirmed by measuring the spiked cereal samples and authentic samples.

## 2. Materials and methods

### 2.1. Materials and reagents

The anti-AFB<sub>1</sub> nanobody named Nb26 was prepared in our previous study (He et al., 2022). *E. coli* BL21(DE3) strain and Nb26/pET32m plasmid were stored in our laboratory. All PCR primer synthesis and DNA sequencing were conducted at Tsingke Biotechnology Co., Ltd. (Beijing, China). Restriction enzymes, T4 DNA ligase, and PCR reagents were purchased from Takara Bio Inc. (Dalian, China). The DNA gel extraction kit and plasmid extraction kit were purchased from Axygen

(Suzhou, China). pMal-T-Avi-His/BirA plasmid was purchased from Nova lifetech Inc. (Hongkong, China). Standards of aflatoxins were obtained from J&K Scientific Ltd. (Beijing, China). The AFB<sub>1</sub>-BSA conjugate was purchased from Sigma-Aldrich (St. Louis, MO, USA). Anti-His tag mAb conjugated horseradish peroxidase (anti-His-HRP) was purchased from GenScript (Nanjing, China). Streptavidin conjugated HRP (SA-HRP) was obtained from AmyJet Scientific (Wuhan, China). 3,3',5,5'-tetramethyl benzidine (TMB), D-Biotin, *N*-hydroxysuccinimide (NHS), 1-(3-dimethylaminopropyl)-3-ethylcarbodiimide hydrochloride (EDC), and carboxyl magnetic beads (0.5 μm) were obtained from Sangon Biotech Co. Ltd. (Shanghai, China). HisTrap HP column was purchased from GE Healthcare (Chicago, Illinois, USA). 96-well polystyrene microtiter plates were obtained from Corning Inc. (Kennebunk, ME, USA). All other chemicals and agents used were of analytical grade unless otherwise specified. Optical density (OD) was measured using a SpectraMax i3x microplate reader from Molecular Devices (CA, USA).

## 2.2. Construction of the expression vector of *AviTag-Nb* fusion proteins

All the nucleotide sequences of primers used are listed in Table S1. Recombinant plasmids containing the *AviTag* peptide (GLNDI-FEAQKIEWHE) at different junction sites, encoding three *AviTag-Nb26* fusion proteins (*AviTag-Nb26-His*, *Nb26-AviTag-His*, and *Nb26-His-AviTag*). By using specific primers (Table S1), the *VHH* genes of *Nb26*, along with a flexible peptide linker (Gly<sub>4</sub>Ser) and restriction sites were amplified via PCR (Liu, Chen, et al., 2023). The *AviTag* gene was synthesized and ligated to the *Nb26/pET32m* vector by enzyme digestion and ligation (Mao et al., 2022). The schematic illustration of the production of biotinylated *AviTag-Nb* fusions was shown in Fig. 1A.

Taking the construction of recombinant plasmid *AviTag-Nb26-His/pET32m* as an example, the detailed protocol is as follows. Using NF-1 and NR-1 primers (Table S1), the *Nb26* encoding gene was amplified from plasmid *Nb26/pET32m* by PCR. The NF-1 and NR-1 primers contain *Bam*H I and *Xho* I restriction sites, respectively. The nucleotide that encodes for the linker (Gly<sub>4</sub>Ser) is also included in the forward primer. The DNA oligos (AF-1 and AR-1, listed in Table S1) for sense and antisense strands of *AviTag* gene were respectively synthesized, and then annealed to obtain the double-stranded DNA with different overhang ends. Annealing was accomplished by 10 min of boiling the mixture containing identical molar ratio of sense and antisense strands of *AviTag* gene, and then naturally cooling the liquid to room temperature. The digested *Nb26* DNA and the annealed *AviTag* DNA were mixed in equal molar ratio and then ligated with *pET32m* vector, which had been predigested with *Nde* I and *Xho* I enzymes. The resulting recombinant plasmid *AviTag-Nb26-His/pET32m* was confirmed through DNA sequencing.

## 2.3. Expression, purification, and identification of biotinylated *AviTag-Nb* fusions

The *BirA* encoding gene (*birA*) was amplified from the pMal-T-Avi-His/BirA plasmid using gene-specific primers BF and BR (Table S1). A stop codon was added at the end of *birA* to ensure that the enzyme was expressed without a His-tag. After digestion with *Nco* I and *Sal* I, the resulting *birA* gene was inserted into the *pET28a* vector, which had been doubly digested with the same enzymes. The resulting plasmid *BirA/pET28a* was confirmed by DNA sequencing. To produce three biotinylated *AviTag-Nb* fusions, each of the *AviTag-Nb* recombinant plasmid was transformed into *E. coli* BL21(DE3) cells harboring the *BirA/pET28a* plasmid, enabling *Nbs* to be biotinylated during expression (Chen et al., 2022).

The *E. coli* cells containing the above plasmids were grown in LB broth supplemented with 100 μg/mL ampicillin and 50 μg/mL kanamycin at 37 °C until the OD<sub>600</sub> reached 0.6. Subsequently, a final concentration of 0.5 mmol/L isopropyl-β-D-thiogalactopyranoside (IPTG) and 200 μmol/L D-biotin were added to induce the expression and

biotinylation of *AviTag-Nb* fusion proteins at 20 °C for 12 h. The bacterial cells were collected by centrifugation and lysed by sonication. The lysate was clarified by centrifugation at 20000 rpm for 30 min. The supernatant was purified using the ÄKTApurify™ chromatography system (GE Healthcare) with a HisTrap HP column. After repeated dialysis against PBS buffer at 4 °C, the concentration of purified biotinylated *AviTag-Nb* fusions was quantified using a NanoPhotometer (Implen, Munich, Germany), and their purity was assessed by 15% reducing SDS-PAGE. The dual function of the biotinylated *AviTag-Nb26* fusions with AFB<sub>1</sub>-binding activity and streptavidin-binding activity was identified by indirect competitive ELISA (icELISA) with SA-HRP as the detection tracer (Liu, He, et al., 2023).

## 2.4. Development of BA-ELISA and MB-ELISA based on biotinylated *AviTag-Nb* fusion

The BA-ELISA protocol was performed according to the method described by Yan et al. (Yan et al., 2022). Briefly, a 96-well microtiter plate was coated with AFB<sub>1</sub>-BSA (1.0 μg/mL, 100 μL/well) overnight at 4 °C, followed by blocking with 4% skim milk at 37 °C for 1 h. After discarding the blocking solution, the plate was washed three times with PBST (PBS containing 0.05% Tween 20). Diluted biotinylated *AviTag-Nb26-His* (50 μL/well) and serially diluted AFB<sub>1</sub> standard solution (50 μL/well) were added. The plate was incubated for 20 min at 37 °C, washed three times, and then supplied with 100 μL/well of SA-HRP in PBST for another 20 min of reaction. After six washes, 100 μL/well of TMB substrate was added and incubated at 37 °C for 10 min. The chromogenic reaction was stopped by adding 50 μL/well of 2 mol/L H<sub>2</sub>SO<sub>4</sub>, and the optical density at 450 nm (OD<sub>450</sub>) was measured by a microplate reader. The standard curve for BA-ELISA was obtained by plotting the B/B<sub>0</sub> (where B and B<sub>0</sub> represent the OD<sub>450</sub> in the presence and absence of AFB<sub>1</sub>, respectively) against the logarithm of AFB<sub>1</sub> concentration.

To construct the MB-ELISA method, the initial step involves preparing the AFB<sub>1</sub> antigen-magnetic probe (MBs-AFB<sub>1</sub>-BSA). This is achieved by coupling carboxyl functionalized magnetic beads (MBs) with AFB<sub>1</sub>-BSA using the NHS/EDC method (Li et al., 2022), following the instructions provided by the supplier (Sangon, Shanghai, China; D601013). 300 μL of ultrasonically dispersed MBs (50 mg/mL) were washed three times with activation buffer. Subsequently, the MBs were incubated with 100 μL of NHS (50 mg/mL) and 100 μL of EDC (50 mg/mL) for 15 min. They were then separated using a magnetic field and resuspended in 2 mL of coupling buffer. AFB<sub>1</sub>-BSA in the coupling buffer was mixed with the activated MBs and incubated for 2 h with vigorous shaking. After magnetic separation, the MBs were blocked with 5 mL of blocking buffer for 30 min and then dispersed in 2 mL of storage buffer to obtain MBs-AFB<sub>1</sub>-BSA. Finally, fluorescence spectra measurements were performed to characterize MBs, AFB<sub>1</sub>-BSA, and MBs-AFB<sub>1</sub>-BSA.

The MB-ELISA was conducted following the protocol of Zuo et al. (Zuo, Wang, et al., 2023) with minor modifications. In brief, a 96-well microplate was blocked with 4% skim milk and incubated at 37 °C for 1 h. After washing with PBST, 15 μg of MBs-AFB<sub>1</sub>-BSA, 50 μL of serially diluted AFB<sub>1</sub> standard solution, and 50 μL of diluted biotinylated *AviTag-Nb26-His* solution were mixed into the wells. The plate was then incubated at 37 °C for 10 min and placed on a magnetic base to precipitate the complex of MBs-AFB<sub>1</sub>-BSA-biotinylated *Nb26*. After magnetic separation and washing with PBST, the plate was supplied with 100 μL/well of SA-HRP in PBST for 8 min of reaction at 37 °C. Following another separation and washing step, 100 μL of the substrate TMB was added and incubated for another 8 min at 37 °C. The chromogenic reaction was stopped with 2 mol/L H<sub>2</sub>SO<sub>4</sub>, and the OD<sub>450</sub> was measured. The standard curve plotting for MB-ELISA was the same as that of BA-ELISA above.

## 2.5. Optimization, sensitivity, and selectivity of BA-ELISA and MB-ELISA

The assay sensitivity was greatly affected by reaction conditions (Cai et al., 2023). Thus, several experimental parameters including concentrations of coating antigen AFB<sub>1</sub>-BSA (or MBs-AFB<sub>1</sub>-BSA) and biotinylated AviTag-Nb26-His, ionic strength, pH value, organic solvent content in buffer, and incubation time were investigated to improve the sensitivity of immunoassays. The optimal conditions were determined, and the data was evaluated using the Origin 8.0 software (Origin Lab, Northampton, ME) to establish standard curves with a four-parameter logistic equation. The 50% inhibitory concentration value (IC<sub>50</sub>) calculated from the curves was used to evaluate the sensitivity of the assays.

Additionally, cross-reactivities (CRs) for compounds structurally similar to AFB<sub>1</sub> were used to evaluate the specificity of the assays. The CR values were calculated as follows: CR (%) = (IC<sub>50</sub> of AFB<sub>1</sub>/IC<sub>50</sub> of analogs) × 100%.

## 2.6. Sample analysis and validation

The preparation and extraction of the cereal samples were described as follows (Yan et al., 2022). Briefly, 5 g of milled cereal samples (wheat and corn), shown to be AFB<sub>1</sub> free by HPLC, were weighed into 50 mL centrifuge tubes. Then, 15 mL of 70% methanol-water (v/v) solution was added to each tube. The mixture was thoroughly mixed on a vortex for 20 min and then centrifuged at 5000 g for 5 min. The resulting supernatant was collected and filtered through a 0.22 μm filter for further analysis using BA-ELISA and MB-ELISA. Four naturally contaminated cereal samples collected from different parts of China were treated in the same manner.

The sample preparation for HPLC analysis followed the protocol described by Li et al. (Li et al., 2019) with slight modifications. Briefly, 5.0 mL of the extraction supernatant was transferred to a clean centrifuge tube and diluted with 15.0 mL of water. Then, 12.0 mL of the diluted solution was loaded onto an immunoaffinity chromatography column (Cusabio, Wuhan, China). The AFB<sub>1</sub> was eluted with 1.0 mL of methanol and collected in a 2.0 mL brown vial, then injected into an HPLC system equipped with a fluorescence detector. The mobile phase consisted of a mixture of HPLC-grade methanol-water (55:45) flowing at a rate of 1.0 mL/min. The injection volume was 10.0 μL, and the signal (λ<sub>em</sub>: 440 nm) was recorded at an excitation wavelength of 360 nm.

## 2.7. Statistical analysis

All measurements were performed twice. One-way analysis of variance (ANOVA) was conducted using R software to evaluate the statistical significance of the data at  $P < 0.05$ .

## 3. Results and discussion

### 3.1. Expression, purification, and characterization of the biotinylated AviTag-Nb fusions

The biotin-streptavidin binding has been extensively used in bio-analytical research, because of the strong noncovalent interaction and high specificity (Sun et al., 2019). In this study, the AviTag/BirA technology was employed to obtain *in vivo* biotinylated Nbs in *E. coli* (Chen et al., 2022). The schematic illustration of the production of biotinylated AviTag-Nb fusions was outlined in Fig. 1A. Firstly, considering that the relative position of the tagged peptide may affect the functional binding activity of recombinant chimeras (Liu, Chen, et al., 2023), Nbs were fused with AviTag at three different junction sites to construct the recombinant plasmids of AviTag-Nb26-His, Nb26-AviTag-His, and Nb26-His-AviTag. Subsequently, these three recombinant plasmids were separately co-transformed with plasmid BirA/pET28a into *E. coli* BL21 (DE3) competent cells to coexpress the AviTag-Nb fusions and BirA. Colony PCR was performed to confirm the presence of both plasmids in

each *E. coli* cell. The amplified fragments of AviTag-Nb gene (approximately 550 bp) and BirA gene (approximately 1100 bp) were subsequently confirmed by DNA agarose gel electrophoresis, as seen in Fig. 1B.

The expression of three biotinylated AviTag-Nb fusions was characterized through SDS-PAGE analysis (Fig. 1C). The analysis revealed a clear single target band of approximately 18 kDa for the biotinylated AviTag-Nb fusions (Fig. 1C, Lanes 4, 7, and 10), which was obviously larger than that of non-biotinylated Nb26 (Fig. 1C, Lane 1). This due to the specific recognition between the AviTag in the recombinant vector and biotin. In addition, the presence of the overexpressed BirA enzyme with a molecular weight of 36 kDa was also observed in all three induced cells (Lanes 3, 6, and 9 in Fig. 1C), which ensures the completion of biotinylation of AviTag-Nb fusions in *E. coli*. The yields of AviTag-Nb26-His, Nb26-AviTag-His, and Nb26-His-AviTag were calculated to be 1.9, 0.95, and 1.1 mg/L, respectively.

As shown in Fig. 1D, ELISA testing was conducted to further demonstrate the activity and specificity of three biotinylated AviTag-Nb fusions, which were found to be similar to non-biotinylated Nb26 (He et al., 2014). This indicated that their functional properties were not influenced by biotinylation. Among the tested fusion proteins, AviTag-Nb26-His exhibited a lower IC<sub>50</sub> value (0.77 ng/mL) compared to Nb26-AviTag-His (1.46 ng/mL) and Nb26-His-AviTag (0.84 ng/mL), suggesting that AviTag-Nb26-His had better sensitivity. The differences in sensitivity among the AviTag-Nb fusions imply that tethering AviTag to the N-terminus of Nb26 is more favorable for retaining the AFB<sub>1</sub>-binding activity of the original Nb26. These findings are consistent with our previous research on the recognition mechanism of Nb26 binding to AFB<sub>1</sub>, where the active pocket of Nb26 is located near its C-terminus (He et al., 2022). Therefore, fusing AviTag at the C-terminus may increase steric hindrance of Nb26 to bind AFB<sub>1</sub> or partially alter the conformation of antibody's active pocket, resulting in a relatively lower affinity of the antibody for the ligand. These results evidenced the successful biotinylation of AviTag-Nb26 fusions and supported the preference for using biotinylated AviTag-Nb26-His in the detection method development.

Generally, Nbs possess great physiochemical stability under harsh conditions. In this study, the effects of various organic solvents on the binding activity of biotinylated AviTag-Nb26-His were investigated. Fig. S1 shows that the binding activity of biotinylated AviTag-Nb26-His remained at no less than 77.4% when the solvent concentration ranged from 0% to 40% for methanol, ethanol, dimethylformamide (DMF), acetonitrile, and acetone. However, the binding activity decreased to 46.4% with increasing dimethylformamide (DMF) concentration up to 30%, but then increased to 96.5% when the DMSO concentration reached 40%. These findings suggested that biotinylated AviTag-Nb26-His exhibits a high tolerance to the evaluated solvents, possibly due to the stable conformation of the Nb's binding pocket in the presence of high organic solvent content (He et al., 2022). Consequently, the high organic tolerance of biotinylated AviTag-Nb26-His allows for its use in sample pretreatment without requiring extensive dilution.

### 3.2. Development and optimization of BA-ELISA

In order to assess the applicability of AviTag-Nb in immunoassay, a biotin-streptavidin-amplified ELISA (BA-ELISA) was initially developed using the biotinylated AviTag-Nb26-His as the capture antibody and SA-HRP as the detection tracer. Various parameters that can influence the detection sensitivity of BA-ELISA were optimized through single-factor tests, including the concentration of coating antigen AFB<sub>1</sub>-BSA (0.125, 0.25, 0.5, 1.0, 2.0, and 4.0 μg/mL), biotinylated AviTag-Nb26-His (0.02, 0.03, 0.05, 0.1, 1.0, and 1.5 μg/mL), blocking reagents (1.5% BSA, 1.5% OVA, and 4% skim milk), competitive reaction time (20, 40, and 60 min), SA-HRP incubation time (20, 40, and 60 min), methanol concentration (5, 10, 15, and 20%), pH value (6.0, 7.0, 7.4, 8.0, and 9.0) and ionic strength (10, 20, 40, 80, and 160 mmol/L). The optimization

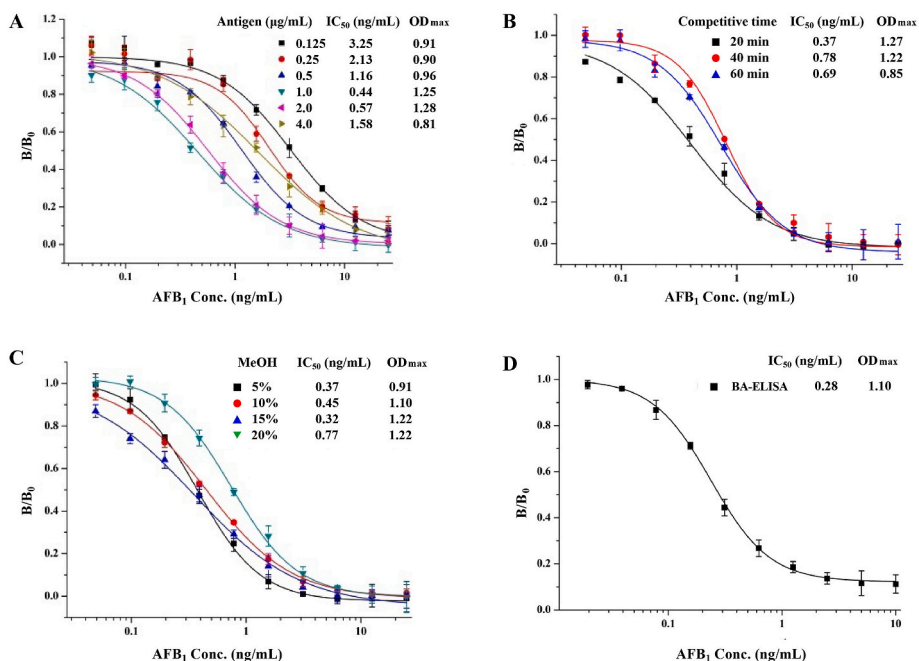


**Fig. 2.** Influence of different parameters on the performance of BA-ELISA. (A) Coating antigen and biotinylated AviTag-Nb26-His concentration. (B) Competitive reaction time. (C) Methanol concentration. (D) Standard curve of BA-ELISA. Each point represents the mean of three replicates.

evaluation criteria were based on the maximum absorbance value (OD<sub>max</sub>) of negative control and the lowest IC<sub>50</sub> value. The best working conditions for further analysis were determined to be 1.0 μg/mL of AFB<sub>1</sub>-BSA, 0.05 μg/mL of biotinylated AviTag-Nb26-His, blocking reagent containing 4% skim milk, 20 min of competitive time, 20 min of SA-HRP incubation time, 15% methanol content, pH 8.0, and 40 mmol/L NaCl (Fig. 2 and Fig. S2).

Under optimal conditions, a standard curve for the AviTag-Nb-based BA-ELISA was developed at various concentrations of AFB<sub>1</sub>. As presented in Fig. 2D, the sensitivity (IC<sub>50</sub>) of BA-ELISA was determined to be 0.28 ng/mL, which was 2.7-fold higher than that of conventional

ELISA (IC<sub>50</sub> = 0.75 ng/mL) (He et al., 2014). Furthermore, the assay exhibited a detection limit (LOD = IC<sub>10</sub>) of 0.07 ng/mL and a linear range (IC<sub>20</sub>-IC<sub>80</sub>) of 0.12–0.95 ng/mL. Additionally, the detection procedure for sample analysis was shortened to 50 min compared to the 135 min required for conventional ELISA (He et al., 2014). The successful establishment of the BA-ELISA method showed that the combination of biotinylated AviTag-Nb and SA-HRP formed a biotin-streptavidin amplification system, which could accelerate the immunoreaction and gather more enzyme molecules for substrate catalytic reaction, thereby enhancing the analytical performance of the immunoassay (Sun et al., 2019).

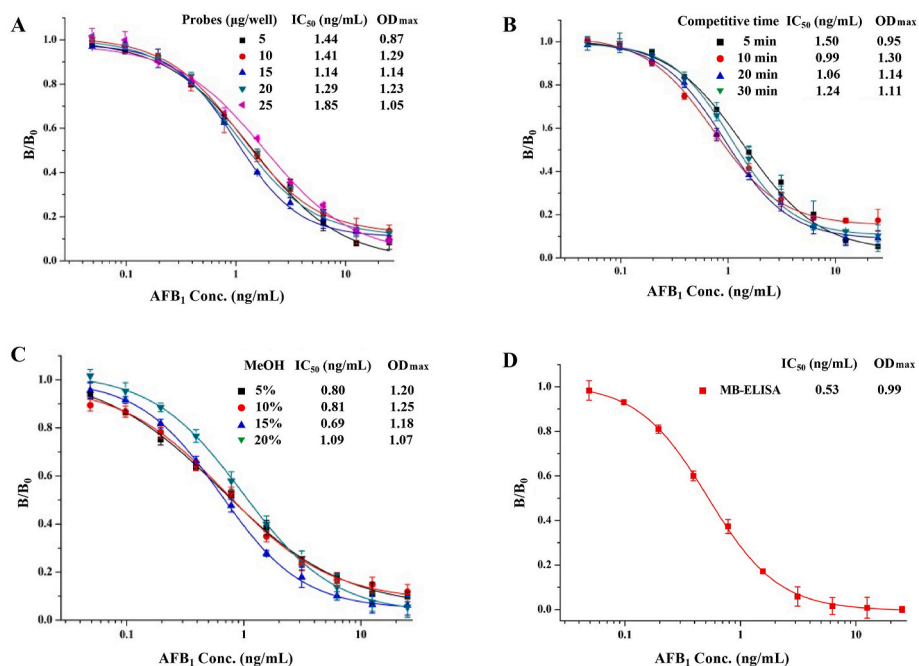


**Fig. 3.** Influence of different parameters on the performance of MB-ELISA. (A) Amount of MBs-AFB<sub>1</sub>-BSA and biotinylated AviTag-Nb26-His concentration. (B) Competitive reaction time. (C) Incubation time of SA-HRP. (D) Standard curve of MB-ELISA. Each point represents the mean of three replicates.

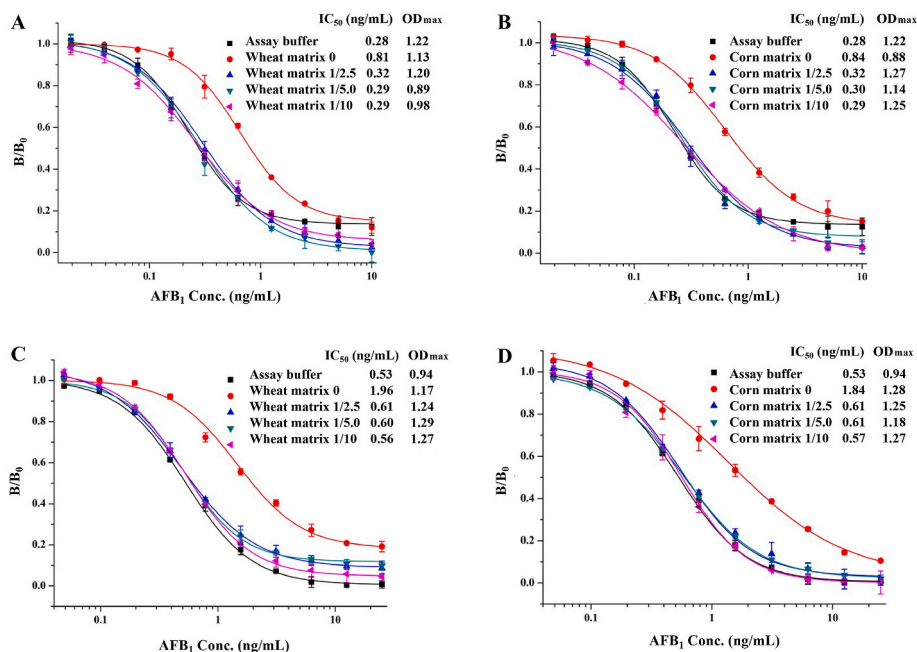


**Fig. 4.** Standard curves of BA-ELISA for AFB<sub>1</sub> in wheat extract (A), and corn extract (B), and MB-ELISA for AFB<sub>1</sub> in wheat extract (C), and corn extract (D). Each point represents the mean of three replicates.

### 3.3. Development and optimization of MB-ELISA

To simplify the BA-ELISA process and broaden the practical application of AviTag-Nb in rapid screening of AFB<sub>1</sub>, magnetic beads (MBs) were utilized as the solid phase. Compared to microplate-based ELISA, the MB-based enzyme immunoassay offers several advantages such as easy operation, fast speed, high flexibility, and good portability (Zuo, Wang, et al., 2023). The first step in establishing MB-ELISA involves preparing antigen-coated MBs. To optimize the process, different amounts of AFB<sub>1</sub>-BSA (10, 30, 50, 70, and 90 µg/mg) were coupled onto the surface of 20 µg MB to create MBs-AFB<sub>1</sub>-BSA. The effect of AFB<sub>1</sub>-BSA immobilization on MBs was evaluated using indirect ELISA (Fig. S3A). The results showed that 50 µg/mg of AFB<sub>1</sub>-BSA reached the saturation point and was therefore selected for synthesizing MB-antigen probes for subsequent studies. Additionally, the fluorescence spectra of MBs-AFB<sub>1</sub>-BSA and AFB<sub>1</sub>-BSA conjugate were measured as AFB<sub>1</sub> has intrinsic fluorescence (Shu, Wu, Wang, & Fu, 2019). Upon excitation at 365 nm, MBs-AFB<sub>1</sub>-BSA and AFB<sub>1</sub>-BSA exhibited maximum emission peaks at 446 nm and 458 nm, respectively. In contrast, bare MBs showed no emission peaks, confirming the successful formation of MBs-AFB<sub>1</sub>-BSA (Fig. S3B).

The optimization process parameters for MB-ELISA were similar to BA-ELISA. The groups of combined MBs-AFB<sub>1</sub>-BSA and biotinylated AviTag-Nb26-His were determined using a checkerboard titration, as shown in Table S3. After optimization, the optimal concentrations for MB-ELISA were determined to be 15 µg/well of MBs-AFB<sub>1</sub>-BSA and 0.2 µg/mL of biotinylated AviTag-Nb26-His (Fig. 3A). The optimal operation time for MB-ELISA was found to be only 10 min for the competitive reaction (Fig. 3B), 8 min for SA-HRP incubation, and 8 min for TMB reaction (Figs. S4A and B). In addition, the lowest IC<sub>50</sub> value was observed at 15% methanol-PBS in MB-ELISA (Fig. 3C), and the best performance buffer for MB-ELISA was found at 20 mmol/L PBS in pH 7.4 (Figs. S4C and D). Under ultimate conditions, the standard inhibition curve of AviTag-Nb-based MB-ELISA was established (Fig. 3D). The developed method exhibited an IC<sub>50</sub> of 0.53 ng/mL and an LOD of 0.12 ng/mL, with a linear detection range (IC<sub>20</sub>-IC<sub>80</sub>) of 0.21–1.37 ng/mL. Unexpectedly, we observed that the detection sensitivity of MB-ELISA did not show further improvement compared to BA-ELISA. This may be attributed to unknown factors that affect the assay performance, such

as the blocking reagents used to react with the excess free amino groups on the MBs surface, which need further optimization (Ecke, Westphalen, Hornung, Voetz, & Schneider, 2022). On the other hand, the detection process from sample addition to result acquisition by MB-ELISA was significantly reduced to 26 min. This reduction in time is mainly due to the use of MBs as an immobile phase, allowing the immunoreaction to occur in solution. This accelerates the separation and enrichment of analytes from complex solutions with the aid of magnetic adhesion, thus enhancing the capture efficiency (Zuo, Wang, et al., 2023).

To summarize, both AviTag-Nb-based BA-ELISA and MB-ELISA showed improved detection sensitivity and reduced time requirements compared to unfused Nb26-based ELISA. Therefore, they have great potential for the sensitive and rapid detection of low concentrations of AFB<sub>1</sub> in foodstuffs.

### 3.4. Selectivity of BA-ELISA and MB-ELISA

Specific recognition is an essential factor for the detection of AFB<sub>1</sub>. To evaluate the selectivity of the two developed methods, four structural analogs of AFB<sub>1</sub> (AFB<sub>2</sub>, AFG<sub>1</sub>, AFG<sub>2</sub>, and AFM<sub>1</sub>) were tested by BA-ELISA and MB-ELISA. The chemical structures of the AFB<sub>1</sub> analogs and the corresponding cross-reactivity (CR) results were listed in Table S4. The results showed that the CR with the AFB<sub>1</sub> analogs obtained by BA-ELISA was less than 5%, and those obtained by MB-ELISA was less than 4%. This indicated that the interference of other AFs in the detection of AFB<sub>1</sub> was negligible. Interestingly, the proposed assays demonstrated significantly improved selectivity in AFB<sub>1</sub> analysis compared to conventional ELISA, which exhibited a higher CR of 10.75% with AFM<sub>1</sub> (He et al., 2014). This enhancement in selectivity could be attributed to the fine-tuning of Nb folding conformation after gene modification, resulting in a more structurally compact binding with AFB<sub>1</sub> over its analogs. To fully comprehend the underlying mechanism, further investigation using computer-assisted molecular simulation is warranted (Qiu et al., 2022). Overall, the high specificity of the developed assays is promising for practical applications in avoiding false-positive results.

### 3.5. Method validation

To analyze the actual sample, the impact of the sample matrix on the

**Table 1**Recovery analysis of AFB<sub>1</sub> in the spiked samples by BA-ELISA, MB-ELISA, and HPLC.

Cereal sample	Spiked level (µg/kg)	BA-ELISA <sup>a</sup>			MB-ELISA			HPLC		
		mean <sup>b</sup> ± SD <sup>c</sup> (µg/kg)	Recovery (%)	RSD (%)	mean ± SD (µg/kg)	Recovery (%)	RSD (%)	mean ± SD (µg/kg)	Recovery (%)	RSD (%)
wheat	5	4.56 ± 0.35	91.2	7.68	4.61 ± 0.39	92.2	8.46	4.50 ± 0.31	90.0	6.89
	10	9.67 ± 0.82	96.7	8.48	9.72 ± 0.76	97.2	7.82	9.43 ± 0.61	94.3	6.47
	20	19.0 ± 1.16	95.0	6.11	18.6 ± 1.25	93.0	6.72	19.2 ± 1.87	96.0	9.74
corn	5	4.55 ± 0.23	91.0	5.05	4.50 ± 0.18	90.0	4.00	4.48 ± 0.28	89.6	6.25
	10	9.51 ± 0.90	95.1	9.46	9.32 ± 0.98	93.2	10.5	9.40 ± 0.80	94.0	8.51
	20	18.7 ± 1.34	93.5	7.17	18.9 ± 1.61	94.5	8.52	19.2 ± 1.28	96.0	6.67

<sup>a</sup> If the sample concentration exceeds the range of the assays, the samples extraction should be diluted for detection.

<sup>b</sup> Data were average from two repeats.

<sup>c</sup> SD, standard deviation.

detection system was excluded prior. The two negative wheat and corn extracts were diluted to prepare serial concentrations of AFB<sub>1</sub> solution for BA-ELISA and MB-ELISA. From Fig. 4, it can be observed that any negative effects on the sample extracts could be reversed after a 2.5-fold dilution. Under ultimate conditions, the developed BA-ELISA had LODs of 0.52 and 0.46 µg/kg in wheat and corn, and linear detection ranges of 0.89–7.07 and 0.82–7.49 µg/kg in wheat and corn for AFB<sub>1</sub>, respectively. Similarly, the developed MB-ELISA had an LOD of 1.13 µg/kg in wheat with a linear detection range of 1.77–16.1 µg/kg, and an LOD of 1.22 µg/kg in corn with a linear detection range of 1.89–12.3 µg/kg for AFB<sub>1</sub>, respectively. These results comply with the European Union regulatory requirements for AFB<sub>1</sub> in maize (5 µg/kg) and most cereal products (2 µg/kg).

To estimate the practical application of the proposed analytical methods, recovery tests were conducted on wheat and corn samples spiked with three levels of AFB<sub>1</sub> (5, 10, and 20 µg/kg). As presented in Table 1, the average recoveries for BA-ELISA ranged from 91.0% to 96.7%, with a relative standard deviation (RSD) ranging from 5.05% to 9.46%. Similarly, the average recoveries and RSD for MB-ELISA were in the range of 90.0%–97.2% and 4.00%–10.5%, respectively. Moreover, HPLC analysis was employed to validate the accuracy of the developed assays. The measurements obtained through BA-ELISA/MB-ELISA showed a strong correlation with those from HPLC, as evidenced by the statistical *P*-values being greater than 0.05 via ANOVA (Fig. S5). These results indicated the reliability and precision of the two assays in accurately quantifying AFB<sub>1</sub> in cereals. Additionally, four cereal samples (two wheat and two corn samples) naturally contaminated with AFB<sub>1</sub> were subjected to BA-ELISA, MB-ELISA, and HPLC testing. The results, depicted in Table S5, revealed a good correlation between BA-ELISA/MB-ELISA and HPLC. Therefore, the developed AviTag-Nb-based BA-ELISA and MB-ELISA present promising analytical tools for sensitive, simple, and rapid screening of AFB<sub>1</sub> in food.

### 3.6. Comparison of Nb- or Nb-fusion-based enzyme immunoassays for AFB<sub>1</sub> analysis

The single domain nature of Nbs makes them convenient for constructing recombinant chimeric or tagged Nbs, which enables novel developments and improvements in immunodetection. Currently, there have only been a few reported immunoassays based on Nb or Nb-fusion protein for AFB<sub>1</sub> detection. Table S6 provides a comparison of the sensitivity and assay time between this work and previously published enzyme immunoassays (Cao et al., 2016; He et al., 2014; Ren et al., 2019; Zhao et al., 2019). The detection capabilities of BA-ELISA and MB-ELISA are comparable to or even better than some previously reported methods for AFB<sub>1</sub> (Table S6). Moreover, the total analysis time of BA-ELISA and MB-ELISA for real samples is much shorter than other microplate-based enzyme immunoassays. Particularly, MB-ELISA demonstrates characteristics of simple operation and flexible application. This comparison confirms that BA-ELISA and MB-ELISA, based on AviTag-Nb, are favorable enzyme immunoassays for the detection of

AFB<sub>1</sub>. It was hopeful to expand the application of AviTag-Nb in immunoassay development for rapid and sensitive detection of food contaminants. Future work can focus on further improving sensitivity and simplicity of these AviTag-Nb-based immunoassays to make them more effective. This could involve constructing tandem AviTag repeats fused with Nb to generate multivalent biotinylated Nbs, developing AviTag-Nb-based fluorescence immunoassays, or exploring the potential of immunochromatography (Chen et al., 2022; Gao et al., 2022; Liu, He, et al., 2023).

## 4. Conclusions

In this study, we have presented a green biosynthesis approach for constructing biotinylated Nbs, which eliminates the need for coupling reactions and chemical modification in the fabrication of this functional probe. The optimal construct, AviTag-Nb26-His, was successfully utilized to develop BA-ELISA and MB-ELISA methods. After verification, both proposed assays demonstrated enhanced detection sensitivity, selectivity, and rapidity in determining AFB<sub>1</sub> in real samples compared to conventional ELISA. Importantly, these results highlight the potential of the clonable AviTag-Nb as a cost-effective and versatile probe in the development of immunoassays for quantifying AFB<sub>1</sub> and other small chemical contaminants in practical applications.

### CRedit authorship contribution statement

**Ting He:** Conceptualization, Funding acquisition, Methodology, Validation, Writing – review & editing. **Tingting Yan:** Methodology, Validation, Writing – original draft. **Jiang Zhu:** Investigation, Methodology. **Ying Li:** Investigation, Writing – review & editing. **Xin Zhou:** Funding acquisition, Writing – review & editing. **Yunhuang Yang:** Conceptualization, Funding acquisition, Supervision, Writing – review & editing. **Maili Liu:** Writing – review & editing.

### Declaration of competing interest

The authors declare that they have no known competing financial interests or personal relationships that could have appeared to influence the work reported in this paper.

### Data availability

Data will be made available on request.

### Acknowledgements

We thank Prof. Peiwu Li in Oil Crops Research Institute of the Chinese Academy of Agricultural Sciences, for his kindness in providing us with anti-AFB<sub>1</sub> nanobody Nb26. This work was supported by the National Natural Science Foundation of China [grant numbers 21921004, 22074152]; and the Natural Science Foundation of Hubei Province

[grant number 2023AFB527].

## Appendix A. Supplementary data

Supplementary data to this article can be found online at <https://doi.org/10.1016/j.lwt.2024.115858>.

## References

- Cai, C., Liu, Y., Tang, X. Q., Zhang, W., Zhang, Q., & Li, P. W. (2023). Development of a toxin-free competitive immunoassay for aflatoxin M1 based on a nanobody as surrogate calibrator. *LWT-Food Science and Technology*, *182*, Article 114829. Article.
- Cao, D. M., Xu, Y., Tu, Z., Li, Y. P., Xiong, L., & Fu, J. H. (2016). One-step enzyme linked immunosorbent assay for detection of aflatoxin B<sub>1</sub> using a nanobody-alkaline phosphatase fusion protein. *Chinese Journal of Analytical Chemistry*, *44*(7), 1085–1091.
- Chen, M. T., Qileng, A., Liang, H. Z., Lei, H. T., Liu, W. P., & Liu, Y. J. (2023). Advances in immunoassay-based strategies for mycotoxin detection in food: From single-mode immunosensors to dual-mode immunosensors. *Comprehensive Reviews in Food Science and Food Safety*, *22*(2), 1285–1311.
- Chen, Z. J., Zhang, Y. F., Chen, J. L., Lin, Z. S., Wu, M. F., Shen, Y. D., et al. (2022). Production and characterization of biotinylated anti-fenitrothionnanobodies and development of sensitive fluorimunoassay. *Journal of Agricultural and Food Chemistry*, *70*(13), 4102–4111.
- Ecke, A., Westphalen, T., Hornung, J., Voetz, M., & Schneider, R. J. (2022). A rapid magnetic bead-based immunoassay for sensitive determination of diclofenac. *Analytical and Bioanalytical Chemistry*, *414*(4), 1563–1573.
- European Commission. (2010). *Setting maximum levels for certain contaminants in foodstuffs as regards aflatoxins. Commission Regulation No. 165/2010, L50 pp. 8–12*. Official Journal of the European Union.
- Gao, X. Y., Xu, C. M., Zhang, X. K., Li, M. R., Gong, X. M., Yang, H. M., et al. (2022). Development of Fe-specific multi-biotinylated antibodies via photoreactive tandem AviTag repeats for the ultrasensitive determination of ochratoxin A. *Food Control*, *132*, Article 108525. Article.
- Guliy, O. I., Evstigneeva, S. S., & Dykman, L. A. (2023). Recombinant antibodies by phage display for bioanalytical applications. *Biosensors and Bioelectronics*, *222*, Article 114909. Article.
- He, J. X., Ma, S. J., Wu, S., Xu, J. J., Tian, J. S., Li, J., et al. (2020). Construction of immunomagnetic particles with high stability in stringent conditions by site-directed immobilization of multivalent nanobodies onto bacterial magnetic particles for the environmental detection of tetrabromobisphenol-A. *Analytical Chemistry*, *92*(1), 1114–1121.
- He, T., Nie, Y., Yan, T. T., Zhu, J., He, X. L., Li, Y., et al. (2022). Enhancing the detection sensitivity of nanobody against aflatoxin B1 through structure-guided modification. *International Journal of Biological Macromolecules*, *194*, 188–197.
- He, T., Wang, Y. R., Li, P. W., Zhang, Q., Lei, J. W., Zhang, Z. W., et al. (2014). Nanobody-based enzyme immunoassay for aflatoxin in agro-products with high tolerance to cosolvent methanol. *Analytical Chemistry*, *86*(17), 8873–8880.
- Li, G. H., Xu, L., Wu, W. Q., Wang, D., Jiang, J., Chen, X. M., et al. (2019). On-site ultrasensitive detection paper for multiclass chemical contaminants via universal bridge-antibody labeling: Mycotoxin and illegal additives in milk as an example. *Analytical Chemistry*, *91*(3), 1968–1973.
- Li, Z., Yang, C. Q., Lu, W. Y., Chu, Z. H., Zhang, J. W., Li, M., et al. (2022). Ultrasensitive immuno-PCR for detecting aflatoxin B1 based on magnetic separation and barcode DNA. *Food Control*, *138*, Article 109028. Article.
- Li, Z. Q., Zhang, W., Zhang, Q., Li, P. W., & Tang, X. Q. (2023). Self-assembly multivalent fluorescence-nanobody coupled multifunctional nanomaterial with colorimetric fluorescence and photothermal to enhance immunochromatographic assay. *ACS Nano*, *17*(19), 19359–19371.
- Liang, Y. F., Zeng, Y. Y., Luo, L., Xu, Z. L., Shen, Y. D., Wang, H., et al. (2022). Detection of acrylamide in foodstuffs by nanobody-based immunoassays. *Journal of Agricultural and Food Chemistry*, *70*, 9179–9186.
- Liu, M. L., Chen, Z. J., Huang, X. Q., Wang, H., Zhao, J. L., Shen, Y. D., et al. (2023a). A bispecific nanobody with high sensitivity/efficiency for simultaneous determination of carbaryl and its metabolite 1-naphthol in the soil and rice samples. *Environmental Pollution*, *335*, Article 122265. Article.
- Liu, M. L., He, X. T., Xu, Z. L., Deng, H., Shen, Y. D., Luo, L., et al. (2023b). Development of a biotinylated nanobody-based gold nanoparticle immunochromatographic assay for the detection of procymidone in crops. *Journal of Agricultural and Food Chemistry*, *71*(35), 13137–13146.
- Liu, X., Wen, Y. P., Wang, W. J., Zhao, Z. T., Han, Y., Tan, K. J., et al. (2020). Nanobody-based electrochemical competitive immunosensor for the detection of AFB1 through AFB1-HCR as signal amplifier. *Microchimica Acta*, *187*(6), Article 352. Article.
- Mao, F. J., Qu, C. S., Li, W. K., He, Z. Y., Pei, H., Sun, Z. C., et al. (2022). Development of a self-assembled heptameric nanobody/streptavidin-binding peptide fusion for ultrasensitive detection of serum biomarkers. *Microchemical Journal*, *181*, Article 107723. Article.
- Muylderms, S. (2021). Applications of nanobodies. *Annual Review of Animal Biosciences*, *9*, 401–421.
- Okechukwu, V. O., Adelusi, O. A., Kappo, A. P., Njobeh, P. B., & Mamo, M. A. (2024). Aflatoxins: Occurrence, biosynthesis, mechanism of action and effects, conventional/emerging detection techniques. *Food Chemistry*, *436*, Article 137775. Article.
- Ostry, V., Malir, F., Toman, J., & Grosse, Y. (2017). Mycotoxins as human carcinogens—the IARC monographs classification. *Mycotoxin Research*, *33*(1), 65–73.
- Qiu, Y. L., You, A. J., Zhang, M. Z., Cui, H. F., Fu, X. S., Wang, J. P., et al. (2022). Phage-displayed nanobody-based fluorescence-linked immunosorbent assay for the detection of Cry3Bb toxin in corn. *LWT-Food Science and Technology*, *171*, Article 114094. Article.
- Ren, W., Li, Z., Xu, Y., Wan, D., Barnych, B., Li, Y., et al. (2019). One-step ultra-sensitive bioluminescent enzyme immunoassay based on nanobody/nano-luciferase fusion for detection of aflatoxin B1 in cereal. *Journal of Agricultural and Food Chemistry*, *67*, 5221–5229.
- Shu, Q., Wu, Y., Wang, L., & Fu, Z. F. (2019). A label-free immunoassay protocol for aflatoxin B1 based on UV-induced fluorescence enhancement. *Talanta*, *204*, 261–265.
- Su, B. C., Xu, H., Xie, G. F., Chen, Q., Sun, Z. C., Cao, H. M., et al. (2021). Generation of a nanobody-alkaline phosphatase fusion and its application in an enzyme cascade-amplified immunoassay for colorimetric detection of alpha fetoprotein in human serum. *Spectrochimica Acta Part A: Molecular and Biomolecular Spectroscopy*, *262*, Article 120088. Article.
- Sun, Z. C., Wang, X. R., Tang, Z. W., Chen, Q., & Liu, X. (2019). Development of a biotin-streptavidin-amplified nanobody-based ELISA for ochratoxin A in cereal. *Ecotoxicology and Environmental Safety*, *171*, 382–388.
- Wang, Y. Z., Chu, L. L., Qu, J. S., Ding, B., & Kang, X. J. (2024). A novel sample pretreatment of nanofiber-packed solid-phase extraction of aflatoxin B1, B2, G1 and G2 in foods and simultaneous determination with HPLC. *Food Chemistry*, *436*, Article 137699. Article.
- Wang, J., Mukhtar, H., Ma, L., Pang, Q., & Wang, X. H. (2018). VHH antibodies: Reagents for mycotoxin detection in food products. *Sensors*, *18*(2), Article 485. Article.
- Wu, S. W., Xu, J. T., Chen, W. X., Wang, F. H., Tan, X. L., Zou, X. L., et al. (2024). Protein nanoscaffold enables programmable nanobody-luciferase immunoassembly for sensitive and simultaneous detection of aflatoxin B1 and ochratoxin A. *Journal of Hazardous Materials*, *462*, Article 132701. Article.
- Yan, T. T., Zhu, J., Li, Y., He, T., Yang, Y. H., & Liu, M. L. (2022). Development of a biotinylated nanobody for sensitive detection of aflatoxin B1 in cereal via ELISA. *Talanta*, *239*, Article 123125. Article.
- Yang, H. L., Zhang, Q., Liu, X. L., Yang, Y. Y., Yang, Y., Liu, M. Y., et al. (2020). Antibody-biotin-streptavidin-horseradish peroxidase (HRP) sensor for rapid and ultra-sensitive detection of fumonisins. *Food Chemistry*, *316*, Article 126356. Article.
- Yoshinari, T., Sugita-Konishi, Y., Sato, E., Takeuchi, H., Taniguchi, M., Fukumitsu, T., et al. (2024). Survey and risk assessment of aflatoxins and sterigmatocystin in Japanese staple food items and the evaluation of an in-house ELISA technique for rapid screening. *Food Control*, *157*, Article 110154. Article.
- Yu, G. G., Wang, J. M., Zhang, Y., Wu, H. F., Wang, Y. Q., Cui, Y., et al. (2023). anti-idiotypic nanobody alkaline phosphatase fusion protein-triggered on-off-on fluorescence immunosensor for aflatoxin in cereals. *Journal of Agricultural and Food Chemistry*, *71*(45), 17391–17398.
- Zhao, F. C., Tian, Y., Shen, Q., Liu, R. X., Shi, R. R., Wang, H. M., et al. (2019). A novel nanobody and mimotope based immunoassay for rapid analysis of aflatoxin B1. *Talanta*, *195*, 55–61.
- Zuo, H., Wang, X. Y., Liu, W. T., Chen, Z. F., Liu, R. N., Yang, H., et al. (2023b). Nanobody-based magnetic chemiluminescence immunoassay for one-pot detection of ochratoxin A. *Talanta*, *258*, Article 124388. Article.
- Zuo, J. S., Yan, T. T., Tang, X. Q., Zhang, Q., & Li, P. W. (2023a). Dual-modal immunosensor made with the multifunction nanobody for fluorescent/colorimetric sensitive detection of aflatoxin B1 in maize. *ACS Applied Materials & Interfaces*, *15*, 2771–2780.